Chaos, Solitons and Fractals 165 (2022) 112778

Contents lists available at ScienceDirect

Chaos, Solitons and Fractals

journal homepage: www.elsevier.com/locate/chaos

The nonequilibrium potential today: A short review☆

H.S. Wio [a,*,1], J.I. Deza [b,1], A.D. Sánchez [c,1], R. García-García [d,1], R. Gallego [e,1], J.A. Revelli [f,1], R.R. Deza [c,1]

[a] IFISC (Instituto de Física Interdisciplinar y Sistemas Complejos), Universitat de les Illes Balears-CSIC, Palma de Mallorca E-07122, Spain
[b] Faculty of Environment and Technology, University of the West of England, Bristol BS16 1QY, UK
[c] IFIMAR, Facultad de Ciencias Exactas y Naturales, Universidad Nacional de Mar del Plata and CONICET, Mar del Plata B7602AYL, Argentina
[d] Department of Physics and Applied Mathematics, Faculty of Sciences, University of Navarra, Pamplona, Spain
[e] Mathematics Department, Gijón Campus, Universidad de Oviedo, Gijón, Spain
[f] IFEG (Instituto de Física Enrique Gaviola), Universidad Nacional de Córdoba and CONICET, FaMAF-UNC, Córdoba, Argentina

ARTICLE INFO

Keywords:
Nonequilibrium potential
Stochastic thermodynamics
KPZ equation

ABSTRACT

A brief review is made of the birth and evolution of the "nonequilibrium potential" (NEP) concept. As if providing a landscape for qualitative reasoning were not helpful enough, the NEP adds a quantitative dimension to the qualitative theory of differential equations and provides a global Lyapunov function for the deterministic dynamics. Here we illustrate the usefulness of the NEP to draw results on stochastic thermodynamics: the Jarzynski equality in the Wilson–Cowan model (a population-competition model of the neocortex) and a "thermodynamic uncertainty relation" (TUR) in the KPZ equation (the stochastic field theory of kinetic interface roughening). Additionally, we discuss system-size stochastic resonance in the Wilson–Cowan model and relevant aspects of KPZ phenomenology like the EW–KPZ crossover and the memory of initial conditions.

1. Introduction

Potential landscapes are a standard tool, taught in basic Physics courses, for qualitative and even some quantitative reasoning. They determine the extent of trajectories in deterministic conservative systems and in 1D, the potential $\Phi(x)$ even determines by quadrature their analytic expression. Not less important are potential landscapes for stochastic dissipative systems: yet whereas some important information (attractors and repellers, local bifurcations) can be retrieved from sheer linearization, some phenomena require the full potential landscape for their description (an instance being excitable behavior). Energy landscapes not only help visualize the systems' phase space and its structural changes as parameters are varied, but allow to predict the rates of activated processes [1–3]. Some fields that benefit from the energy landscape approach are optimization problems [4], neural networks [5], protein folding [6], cell nets [7], gene regulatory networks [8,9], ecology [10], and evolution [11]. The fact that deterministic dissipative systems relax toward their attractors has an expression (known as the "Lyapunov property") in terms of the potential $\Phi(\mathbf{x})$: $\dot{\Phi} < 0$ outside the attractors; $\Phi(\mathbf{x})$ is said to be a "Lyapunov function". Moreover, the framework can also be applied to nonautonomous flows, as far as their explicit time-dependence can be regarded as slow in comparison with the relaxation times toward the system's attractors (adiabatic approximation).

What is less known about potential landscapes in stochastic dissipative systems is that *noise can help meet integrability conditions* in non-integrable deterministic systems. This was shown by Robert Graham and collaborators in a series of works, several of them communicated in successive editions of the International Workshop on Instabilities and Nonequilibrium Structures. They coined the name "nonequilibrium potential" (hereafter, NEP). A convenient classification of dynamical systems is into *potential* and *non-potential* ones, i.e. those which admit a potential and those which do not (this includes systems for which a potential may exist, but it is not known; Hamiltonian systems belong to this class) [12,13]. Graham's finding can thus be restated as follows:

> "*Langevin systems whose Fokker–Planck equation admits a stationary solution are potential*".

Potential systems can in turn be classified into *non-relaxational* and *relaxational*, according to whether a drift component normal to the potential gradient exists or not. A further classification of relaxational

☆ Submitted to "New Trends on Instabilities and Nonequilibrium Structures", issue in memory of Professor Enrique Tirapegui (1940–2020).

* Corresponding author.
E-mail addresses: horacio@ifisc.uib-csic.es (H.S. Wio), Ignacio.Deza@uwe.ac.uk (J.I. Deza), sanchez@mdp.edu.ar (A.D. Sánchez), regarciag@unav.es (R. García-García), rgallego@uniovi.es (R. Gallego), jorge.revelli@unc.edu.ar (J.A. Revelli), deza@mdp.edu.ar (R.R. Deza).

[1] All the authors have contributed equally to the research of the work. Most of the writing was done by R.R. Deza.

https://doi.org/10.1016/j.chaos.2022.112778
Received 20 July 2022; Received in revised form 28 September 2022; Accepted 2 October 2022
Available online 20 October 2022

systems into *gradient* and *non-gradient* ones is still admitted, according to whether an attractor's basin is locally a revolution paraboloid or a generic one.

In Section 2, we briefly sketch Graham's theory of the NEP [14–33], including short discussions and relevant bibliography on some by now "classic" systems admitting a NEP: the complex Ginzburg–Landau equation (CGLE) [13,34–40], the FitzHugh–Nagumo (FHN) model [41–46] and one-component reaction–diffusion systems with field-dependent diffusivity [1,2,47–54]. In Section 3 we introduce two more systems admitting a NEP: (1) The KPZ equation—the stochastic field theory of kinetic interface roughening—has been shown to be a stochastic gradient system [55–62]: the functional it stems from displays the Lyapunov property, even though it is unbound from below and keeps memory of the process. We then understand that an interface's kinetic roughening is a phenomenon akin to that of escape through a barrier (thus losing lower boundedness, although not the Lyapunov property). Among its virtues, it yields a visual criterion for the EW–KPZ crossover. (2) The Wilson–Cowan model of the neocortex—describing the competition between excitatory and inhibitory neural populations—is generically a non-relaxational potential system admitting a *bona-fide* NEP [63]. In Section 4, we illustrate the usefulness of the NEP concept to draw results on stochastic thermodynamics by deriving a Jarzynski equality [64] in the Wilson–Cowan model and a thermodynamic uncertainty relation (TUR) [65] in the KPZ equation. In Section 5, we further illustrate the usefulness of the NEP concept by analyzing the memory of initial conditions in KPZ and system-size stochastic resonance [66] in the Wilson–Cowan model. We close by summarizing our conclusions in Section 6.

2. Graham's theory

2.1. Univariate systems

It is well known that the conditional probability density function (pdf) $P(x,t|x_0,0)$ of an univariate stochastic process $x(t)$ ($t \geq 0$, $x \in \Omega \subset \mathbb{R}$) that obeys a generalized Langevin equation

$$\dot{x} = f(x) + g(x)\,\xi(t), \quad x(0) = x_0 \tag{2.1}$$

when submitted parametrically—via $g(x)$—to a centered Gaussian white noise $\xi(t)$, $\langle \xi(t)\rangle = 0$, $\langle \xi(t)\xi(t')\rangle = 2D\,\delta(t-t')$, obeys in turn a Fokker–Planck equation (FPE)

$$\partial_t P + \partial_x J = 0 \tag{2.2}$$

with

$$J(x,t|x_0,0) := \begin{cases} fP + Dg^2\,\partial_x P \\ (f+gg')P + Dg^2\,\partial_x P \end{cases}$$

according to whether $\int_t^{t+\mathrm{d}t} \mathrm{d}\tau\; g(x(\tau))\xi(\tau)$ is interpreted in prepoint (Itô) or in midpoint (Stratonovich) sense. The standard proof relies on Doob's theorem [3,67], according to which the Kramers–Moyal expansion terminates at the second order if $\xi(t)$ is Gaussian. An alternative and very elegant proof [12,68] resorts to Novikov's theorem [69]. Also, everybody knows that the FPE is an eigenvalue equation $\partial_t P = \lambda P$, $\lambda \leq 0$. Now, the FPE may or may not saturate the $\lambda = 0$ bound. A known instance of the first case is pure diffusion, where the asymptotic normalization of P still depends on t. **If** it does, then there exists a stationary pdf (spdf) $P^{\mathrm{st}}(x)$, independent of x_0. It stems from Eq. (2.2) by setting $J(x,t|x_0,0) = J$, a constant which for Dirichlet or natural boundary conditions will be zero.[2] In such a case, we may write

$$P^{\mathrm{st}}(x) = \frac{\exp[-\Phi(x)/D]}{\int_\Omega \mathrm{d}x\,\exp[-\Phi(x)/D]}, \tag{2.3}$$

with

$$\Phi(x) := -\int_{x_0}^{x} \mathrm{d}y \begin{cases} f/g^2 \\ (f+gg')/g^2 \end{cases}. \tag{2.4}$$

Eq. (2.4) assumes that $g^2 > 0$ or at least, that any singularity of the integrand is a removable one. In such a case, we might have performed the (possibly piecewise) one-to-one transformation $z = \int_{x_0}^{x} \mathrm{d}y/g(y)$ to retrieve a conventional Langevin equation in the field $\Psi(z) := -\int_{z_0}^{z} \mathrm{d}y\, f(y)/g(y)$. We then recover Eq. (2.4) by transforming back. Hence in the following, we can assume that $g(x) = 1$. Then $\Phi(x)$ turns out to be a global Lyapunov function of the deterministic dynamics: $\dot{\Phi} = -\Phi' \dot{x} = -\Phi'^2 < 0$. In each attractor's basin, the latter evolves toward the attractor which on the other hand, is a relative maximum of $P^{\mathrm{st}}(x)$.

2.2. Multivariate systems

Regarding multivariate processes, there is a simple case where $f(x_j) = f(x)$, $1 \leq j \leq n$. As far as the x_j are coupled *linearly*—i.e., through a symmetric "adjacency matrix" (in fact, a quadratic form or tensor)—these so-called *gradient systems* admit a potential, no matter how large n be (this fact is widely known for arrays of harmonic oscillators and linear circuits). Of special interest is the case of *reaction–diffusion* systems (even with *density-dependent diffusion*) to be addressed in Section 3.2.

For nongradient systems, integrability conditions are not granted for the deterministic system. Nonetheless—as Graham and Haken first noticed [14]—some nongradient systems behave as stemming from a NEP. The clue to this puzzle was unveiled by Graham et al. along a series of works [20–31]: a properly conditioned noise correlation matrix (again, a tensor) can eventually help the system meet integrability conditions. What Graham et al. realized more than thirty years ago is that *even in the deterministic limit*, this space enlargement can eventually help meet the integrability conditions.

For an n–component dynamic flow[3]

$$\dot{\mathbf{x}} = \mathbf{f}(\mathbf{x}) + \sigma\,\Xi(t), \tag{2.5}$$

submitted via a constant mobility tensor σ to n Gaussian, centered and uncorrelated white noises $\xi_i(t)$ with common variance D, i.e. $\langle \Xi(t)\rangle = 0$ and $\langle \Xi(t)\,\Xi^T(t')\rangle = 2DI\,\delta(t-t')$, the *nonequilibrium potential* (NEP) has been thus defined [27] as

$$\Phi(\mathbf{x}) = -\lim_{D\to 0} D\,\ln P_{\mathrm{st}}(\mathbf{x};D). \tag{2.6}$$

That implies $P_{\mathrm{st}}(\mathbf{x};D) \propto \exp[-\Phi(\mathbf{x};D)/D] + \mathcal{O}(D)$, which replaced into the stationary n–variable FPE $\nabla\cdot[\mathbf{f}(\mathbf{x})P_{\mathrm{st}}(\mathbf{x}) - D\,Q\,\nabla P_{\mathrm{st}}(\mathbf{x})] = 0$ (with $Q := \sigma\sigma^{\mathrm{T}} = Q^{\mathrm{T}}$) yields in the $\lim_{D\to 0}$ the equation

$$\mathbf{f}^{\mathrm{T}}(\mathbf{x})\nabla\Phi + (\nabla\Phi)^{\mathrm{T}} Q\,\nabla\Phi = 0, \tag{2.7}$$

from which $\Phi(\mathbf{x})$ can in principle be found. In an attractor's basin, asymptotic stability imposes $\det Q = (\det\sigma)^2 > 0$, which in turn requires σ to be nonsingular. Using Eq. (2.7),

$$\dot{\Phi} = \dot{\mathbf{x}}^{\mathrm{T}}\nabla\Phi = \mathbf{f}^{\mathrm{T}}(\mathbf{x})\nabla\Phi = -(\nabla\Phi)^{\mathrm{T}} Q\,\nabla\Phi < 0$$

for $D \to 0$. Hence, $\Phi(\mathbf{x})$ is a *Lyapunov function* for the *deterministic* dynamics. Note that although the setup in Eq. (2.5) looks somewhat artificial (a system coupled to many heat sources in relative equilibrium at "temperature" D) it turns out to be equivalent to the genuinely out-of-equilibrium problem $\dot{\mathbf{x}} = \mathbf{f}(\mathbf{x}) + \Xi(t)$, $\langle \Xi(t)\,\Xi^T(t')\rangle = 2DQ\,\delta(t-t')$.

Like the Hamilton–Jacobi equation, Eq. (2.7) is quadratic in its unknown. This trouble can be circumvented if we can decompose $\mathbf{f}(\mathbf{x}) = \mathbf{d}(\mathbf{x}) + \mathbf{r}(\mathbf{x})$, with $\mathbf{d}(\mathbf{x}) := -Q\,\nabla\Phi$ the *dissipative* part of $\mathbf{f}(\mathbf{x})$. Then Eq. (2.7) reads $\mathbf{r}^{\mathrm{T}}(\mathbf{x})\nabla\Phi = 0$, and $\mathbf{r}(\mathbf{x})$ is the *conservative* part of $\mathbf{f}(\mathbf{x})$. Note that

[2] In the case of periodic boundary conditions (ratchets), J may be a nonzero constant and Eq. (2.3) will become a bit more involved.

[3] Eq. (2.5) generalizes Eq. (2.1) for $g = \mathrm{const}$.

$\mathbf{d}(\mathbf{x})$ is still irrotational (in the sense of the Helmholtz decomposition) but is *not* an exact form (the Hodge decomposition is made in the *enlarged* space).

We may always write $\mathbf{r}(\mathbf{x}) = A\nabla\Phi$, with A antisymmetric (involving $n(n-1)/2$ parameters). For illustration purposes, it suffices to consider $n = 2$, i.e.

$$\mathbf{r}(\mathbf{x}) = \kappa\,\Omega\,\nabla\Phi, \quad \Omega := \begin{pmatrix} 0 & 1 \\ -1 & 0 \end{pmatrix}. \tag{2.8}$$

Now $\mathbf{f}(\mathbf{x}) = -(Q - \kappa\,\Omega)\nabla\Phi$, $\det(Q - \kappa\,\Omega) = \det Q + \kappa^2 > 0$, and thus

$$\nabla\Phi = -(Q - \kappa\,\Omega)^{-1}\mathbf{f}(\mathbf{x}). \tag{2.9}$$

For arbitrary real σ_{ij} we can parameterize

$$\sigma = \begin{pmatrix} \sqrt{\lambda_1}\cos\alpha_1 & \sqrt{\lambda_1}\sin\alpha_1 \\ \sqrt{\lambda_2}\cos\alpha_2 & \sqrt{\lambda_2}\sin\alpha_2 \end{pmatrix}$$

and define $\lambda := \sqrt{\lambda_1\lambda_2}\cos(\alpha_1 - \alpha_2)$ (note that the condition $D > 0$ imposes $\alpha_2 \neq \alpha_1$). Then

$$Q - \kappa\,\Omega = \begin{pmatrix} \lambda_1 & \lambda - \kappa \\ \lambda + \kappa & \lambda_2 \end{pmatrix},$$

and Eq. (2.9) reads

$$\nabla\Phi := \begin{pmatrix} \partial_1\Phi \\ \partial_2\Phi \end{pmatrix} = \tag{2.10}$$

$$-\frac{1}{\det(Q - \kappa\,\Omega)} \begin{pmatrix} \lambda_2 f_1(\mathbf{x}) - (\lambda - \kappa) f_2(\mathbf{x}) \\ -(\lambda + \kappa) f_1(\mathbf{x}) + \lambda_1 f_2(\mathbf{x}) \end{pmatrix}$$

(∂_k is a shorthand for $\partial/\partial x_k$). If a set $\{\lambda_1, \lambda_2, \lambda, \kappa\}$ can be found such that $\Phi(\mathbf{x})$ fulfills the *integrability condition* $\partial_2\partial_1\Phi = \partial_1\partial_2\Phi$, then a NEP exists.

2.3. Stochastic fields

Fields are of course a special case of Section 2.2, in which a subset of the index set refers to a substrate manifold. For instance in $\mathbf{u}(\mathbf{x}, t)$, $\mathbf{u} \equiv \{u_k\}$, $k \in \{1, \ldots, n\}$, whereas $\mathbf{x} \in \mathbb{R}^d$. This hierarchical structure of the index set introduces a great simplification in the formalism of Section 2.2: all one has to do is to substitute, e.g. in Eq. (2.10), $\partial/\partial x_k$ by $\delta/\delta u_k(\mathbf{x})$. This is very convenient since most of the interesting applications of the NEP refer to extended systems. Attractors are now points or curves in *functional space*.

3. Examples, "classic" and new

3.1. Non-extended systems

(a) The FitzHugh–Nagumo system

The voltage-varying conductance model by Hodgkin and Huxley [70] is still nowadays the starting point for "*ab initio*" calculations in neuroscience. In practice however (when such a level of detail is not needed), two-variable reductions which still capture the essential trait of neural, cardiac and other tissues, namely *excitability*, are far more useful. The simplest such reduction is the FitzHugh–Nagumo model [71,72], an activator–inhibitor system for which (in the absence of a tonic current)

$$\mathbf{f}(\mathbf{x}) = \begin{pmatrix} 0 & -1/\epsilon \\ \beta & -1 \end{pmatrix}\mathbf{x} + \begin{pmatrix} g(x_1)/\epsilon \\ 0 \end{pmatrix}, \tag{3.1}$$

$\epsilon := \tau_a/\tau_i \ll 1$ being the ratio of relaxation times. The integrability condition for $\nabla\Phi$ arising from Eq. (2.10),

$$\kappa = -\lambda = -\frac{1}{2}\left(\beta\lambda_1 + \frac{\lambda_2}{\epsilon}\right), \tag{3.2}$$

is fully compatible with the model's bistable and excitable regimes (the ones for which a spdf exists). If for instance we take $\lambda_1 = \mathcal{O}(\epsilon^{-1})$ and $\lambda_2 = \mathcal{O}(\epsilon)$, the restriction becomes $\beta < \epsilon$ [41–46].

(b) Adding linear dissipation to a 1D Hamiltonian system

For nonlinear systems with one degree of freedom having Hamiltonian $H(x,p) := p^2/2m + \tilde{V}(x)$ when undamped, $H(x,p)/\gamma$ is a NEP (for any D) when their damping is linear in p. Denoting $x_1 := x$, $x_2 := p/m$, let γ be the damping per unit mass, and $V(x_1) := \tilde{V}(x_1)/m$. Here $f_1(\mathbf{x}) = x_2$ and $f_2(\mathbf{x}) = -\gamma\,x_2 - V'(x_1)$. The integrability condition yields $\lambda_1 = 0$ (then $\det Q \geq 0$ imposes $\lambda = 0$) and $\lambda_2 = \kappa\gamma$. It turns out that $\mathbf{r}(\mathbf{x}) = \begin{pmatrix} x_2 \\ -V'(x_1) \end{pmatrix}$ and $\nabla\Phi = \kappa^{-1}\begin{pmatrix} V'(x_1) \\ x_2 \end{pmatrix}$, which integrated over any path from $\mathbf{x} = 0$, yields $\Phi(\mathbf{x}) = \kappa^{-1}\left[\frac{x_2^2}{2} + V(x_1)\right]$, so full consistency is achieved for $\kappa = \gamma$. $\mathbf{r}(\mathbf{x})$ is in fact the Hamiltonian flow in $H(\mathbf{x})$, but $\mathbf{f}(\mathbf{x})$ is not Hamiltonian, because $\mathbf{d}(\mathbf{x}) = \begin{pmatrix} 0 \\ -\gamma\,x_2 \end{pmatrix}$.

$\mathbf{r}(\mathbf{x}) \neq 0$ is what violates detailed balance, which in Langevin dynamics is just an expression of $\mathbf{J}^{\rm st}(\mathbf{x}) = 0$. If the turnaround mean frequency given by $\mathbf{r}(\mathbf{x})$ is high enough, this fact can be successfully exploited for slow enough forcing ("adiabatic approximation").

(c) The Hopf normal form

By Eq. (2.6), $\Phi(\mathbf{x})$ is restricted to situations where $P_{\rm st}(\mathbf{x}; D)$ exists. That is *not* the case of generic limit cycles and chaos (although one might start from a spdf, transform to the comobile system where the drift becomes periodic in time and do Floquet analysis on the resulting pdf). However, there is a special case where the treatment becomes simpler: the supercritical Hopf bifurcation near which, the system can be approximated by the Hopf normal form

$$\mathbf{f}(\mathbf{x}) = [A + \mathbf{x}^T\,\mathbf{x}\,B]\,\mathbf{x}, \tag{3.3}$$

$$A = \begin{pmatrix} a_1 & -a_2 \\ a_2 & a_1 \end{pmatrix}, \quad B = \begin{pmatrix} b_1 & -b_2 \\ b_2 & b_1 \end{pmatrix}.$$

In polar coordinates, Eq. (3.3) reads $\dot{r} = a_1\,r + b_1\,r^3$, $\dot{\theta} = a_2 + b_2\,\theta^2$ so in fact, $a_2 = 0$ since the bifurcation is supercritical. Inserting Eq. (3.3) into Eq. (2.10) the Hopf normal form turns out to be potential in the sense defined by Eq. (2.6) only for $b_2 = 0$. Even in this case, $\Phi(\mathbf{x})$ *does* undergo a supercritical Hopf bifurcation from a pointlike attractor toward an extended one. However, the latter does *not* describe a limit cycle but the fact that the deterministic rollover from the destabilized former attractor may equally occur in *any* direction.

Now, recognizing that matrices A, B are representations of complex numbers a, b, one can map $\mathbf{x}$ onto its complex coordinates: $x_1 = (z + z^*)/2$, $x_2 = (z - z^*)/(2i)$, so

$$\dot{z} = f(z, z^*) = zz^*\left(\frac{a}{z^*} + bz\right). \tag{3.4}$$

It is immediate to realize that $f(z, z^*) = -\partial_{z^*}\Phi(z, z^*)$, with

$$\Phi(z, z^*) := -\frac{1}{2}[a\,zz^* + b\,(zz^*)^2].$$

$\Phi(z, z^*) = \Phi(\mathbf{x}^T\mathbf{x})$ turns out to be a real quantity, but $f(z, z^*)$ is not. However, $\Phi(z, z^*)$ *does* describe supercritical limit cycles. In [34], the definition (2.6) was extended to

$$\Phi(z, z^*) = -\lim_{D\to 0} D\,\ln P_{\rm st}(z, z^*; D), \tag{3.5}$$

and $f(z, z^*)$ in (3.4) to

$$f(z, z^*) = -\partial_{z^*}\Phi(z, z^*) + r(z, z^*), \tag{3.6}$$

$$r\,\partial_z\Phi + r^*\partial_{z^*}\Phi = 0. \tag{3.7}$$

(d) The Wilson–Cowan model

This model describes the coevolution of competing populations (coarse-grained activities) x_1, x_2 of *excitatory* and *inhibitory* neurons respectively [73]:

$$\tau_1\,\dot{x}_1 = -x_1 + (\nu_1 - r_1 x_1)s_1(i_1),$$
$$\tau_2\,\dot{x}_2 = -x_2 + (\nu_2 - r_2 x_2)s_2(i_2).$$

The τ_k and r_k are relaxation and refractory times respectively, and the ν_k set the scale of the monotonically increasing (sigmoidal) *response functions* $s_k(i_k)$. In [73], the

$$s_k(i_k) := \frac{1}{1+\exp[-\beta_k(i_k - i_k^0)]} - \frac{1}{1+\exp(\beta_k i_k^0)}$$

are such that $s_k(0) = 0$, and range from $-[1+\exp(\beta_k i_k^0)]^{-1}$ for $i_k \to -\infty$ to $1-[1+\exp(\beta_k i_k^0)]^{-1}$ for $i_k \to \infty$. So the first crucial observation about the model is that it is *asymptotically linear*.

The currents i_k are in turn linearly related to the x_k:

$$\mathbf{i}(\mathbf{x}) := J\mathbf{x} + \mathrm{M} = \begin{pmatrix} j_{11} & -j_{12} \\ j_{21} & -j_{22} \end{pmatrix} \begin{pmatrix} x_1 \\ x_2 \end{pmatrix} + \begin{pmatrix} \mu_1 \\ \mu_2 \end{pmatrix}.$$

All the parameters are real and moreover, the j_{kl} are positive (j_{11} and j_{22} are recurrent interactions, j_{12} and j_{21} are cross-population interactions). The above definitions are such that for $\mathrm{M} = 0$, $\mathbf{x} = 0$ is a stable fixed point. To avoid confusions in the following, note that $\det J = -(j_{11}j_{22} - j_{12}j_{21})$.

In practice however, the names of Wilson and Cowan are associated to the broader class of rate models. In the following we shall show that the model defined by

$$\tau_1 \dot{x}_1 = -x_1 + s_1(i_1), \quad \tau_2 \dot{x}_2 = -x_2 + s_2(i_2) \tag{3.8}$$

does admit a NEP—for *any* functional forms of the nonlinear single-variable functions $s_k(i_k)$[4]—provided global stability is assured.

For the model defined by Eqs. (3.8), it is

$$\mathbf{f}(\mathbf{x}) = \begin{pmatrix} \frac{1}{\tau_1}[-x_1 + s_1(i_1)] \\ \frac{1}{\tau_2}[-x_2 + s_2(i_2)] \end{pmatrix}.$$

The condition $\partial_2\partial_1\Phi = \partial_1\partial_2\Phi$, namely

$$\frac{\lambda_2}{\tau_1}\left[-j_{12}\, s_1'(i_1)\right] - \frac{\lambda-\kappa}{\tau_2}\left[-1 - j_{22}\, s_2'(i_2)\right] =$$
$$-\frac{\lambda+\kappa}{\tau_1}\left[-1 + j_{11}\, s_1'(i_1)\right] + \frac{\lambda_1}{\tau_2}\left[j_{21}\, s_2'(i_2)\right],$$

boils down to

$$j_{12}\,\lambda_2 = j_{11}\,(\lambda+\kappa),\ j_{22}\,(\lambda-\kappa) = j_{21}\,\lambda_1,\ \frac{\lambda-\kappa}{\tau_2} = \frac{\lambda+\kappa}{\tau_1}$$

(and these in turn to $j_{21}\,j_{11}\,\tau_1\,\lambda_1 = j_{12}\,j_{22}\,\tau_2\,\lambda_2$) so that λ_2, λ and κ can be expressed in terms of λ_1, which sets the global scale of $\Phi(\mathbf{x})$:

$$\lambda_2 = \frac{j_{21}}{j_{22}}\frac{j_{11}}{j_{12}}\frac{\tau_1}{\tau_2}\,\lambda_1,\ \lambda = \frac{j_{21}}{j_{22}}\frac{\tau_1+\tau_2}{2\tau_2}\,\lambda_1,\ \kappa = \frac{j_{21}}{j_{22}}\frac{\tau_1-\tau_2}{2\tau_2}\,\lambda_1.$$

Since $\mathbf{r}(\mathbf{x}) = \kappa\,\Omega\,\nabla\Phi$, $\tau_1 = \tau_2$ suffices to render the flow *purely dissipative* (albeit not gradient). From this, a good choice is $\lambda_1 := \frac{j_{22}}{j_{21}}\tau_2\rho$. In summary,

$$Q - \kappa\,\Omega = \rho\begin{pmatrix} \frac{j_{22}}{j_{21}}\tau_2 & \tau_2 \\ \tau_1 & \frac{j_{11}}{j_{12}}\tau_1 \end{pmatrix},$$

$$\det(Q - \kappa\,\Omega) = -\frac{\rho^2\tau_1\tau_2}{j_{12}j_{21}}\det J,$$

and Eq. (2.10) becomes

$$\nabla\Phi = \frac{j_{12}j_{21}}{\rho\tau_1\tau_2\det J}\times \begin{pmatrix} \frac{j_{11}}{j_{12}}[-x_1 + s_1(i_1)] - [-x_2 + s_2(i_2)] \\ -[-x_1 + s_1(i_1)] + \frac{j_{22}}{j_{21}}[-x_2 + s_2(i_2)] \end{pmatrix}. \tag{3.9}$$

Integrating Eq. (3.9) over any path from $\mathbf{x} = 0$, yields

$$\Phi(\mathbf{x}) = -\frac{j_{11}j_{21}x_1^2 - 2j_{12}j_{21}x_1x_2 + j_{12}j_{22}x_2^2}{2\rho\tau_1\tau_2\det J} + \frac{j_{21}\left[S_1(i_1) - S_1(\mu_1)\right] - j_{12}\left[S_2(i_2) - S_2(\mu_2)\right]}{\rho\tau_1\tau_2\det J}. \tag{3.10}$$

As already pointed out, being $s_k(i_k)$ sigmoidal functions, Eq. (3.10) is *at most quadratic*. Global stability thus imposes $\det J < 0$, i.e. $j_{11}j_{22} > j_{12}j_{21}$. But note that matrix J also determines the paraboloid's cross section. For the remaining terms, we note that Eq. (3.9) can be written as

$$\nabla\Phi = \frac{1}{\rho\tau_1\tau_2\det J}\begin{pmatrix} j_{21} & 0 \\ 0 & -j_{12} \end{pmatrix} J(\mathbf{x} - \mathbf{s})$$

and recall that $s_k(i_k)$ have sigmoidal shape. So at large $|\mathbf{x}|$, the component

$$-\frac{1}{\rho\tau_1\tau_2\det J}\begin{pmatrix} j_{21} & 0 \\ 0 & -j_{12} \end{pmatrix} J\mathbf{s}$$

will tend to different constants (according to the signs of i_k), so the asymptotic contribution of these terms will be piecewise linear, namely a collection of half planes.

A popular choice for the response functions is

$$s_k(i_k) := \frac{\nu_k}{2}(1 + \tanh\beta_k i_k), \quad \beta_k > 0,$$

for which

$$S_k(i_k) - S_k(\mu_k) = \frac{\nu_k}{2}\left[i_k - \mu_k + \beta_k^{-1}\ln\frac{\cosh\beta_k i_k}{\cosh\beta_k\mu_k}\right]. \tag{3.11}$$

Its $\beta_k \to \infty$ limit, $\nu_k\,\theta(i_k)$ with

$$S_k(i_k) - S_k(\mu_k) = \nu_k\left[i_k\,\theta(i_k) - \mu_k\,\theta(\mu_k)\right], \tag{3.12}$$

highlights the cores of the response functions while keeping the global landscape. In this case, the second term in Eq. (3.10) is nonetheless than a collection of half planes, which favors geometric reasoning. For example, let us see the mechanism whereby Eqs. (3.8) sustain bistability.

- For $\mu_k < 0$ ($k = 1,2$), there is no question that $\mathbf{x} = 0$ is a fixed point (we may call it the "off" node); Eq. (3.10) reduces to its first term and $\Phi(0) = 0$.
- By suitably choosing the half planes—taking advantage of the relative sign in the numerator of the second term in Eq. (3.10)—another fixed point $\mathrm{N} := (\nu_1, \nu_2)^T$ (the "on" node) can be induced[5] if $(J\mathrm{N})_k > -\mu_k$, $k = 1,2$ (namely $j_{11}\nu_1 - j_{12}\nu_2 > -\mu_1$, $j_{21}\nu_1 - j_{22}\nu_2 > -\mu_2$) with

$$\Phi(\mathrm{N}) = \frac{j_{11}j_{21}\nu_1^2 - 2j_{12}j_{21}\nu_1\nu_2 + j_{12}j_{22}\nu_2^2}{2\rho\tau_1\tau_2\det J} + \frac{j_{21}\nu_1\mu_1 - j_{12}\nu_2\mu_2}{\rho\tau_1\tau_2\det J}.$$

If μ_1 is varied (as in [73,74]), equistability is achieved for

$$\mu_1 = \frac{1}{2}\left[\frac{j_{12}\nu_2}{j_{21}\nu_1}(j_{21}\nu_1 - j_{22}\nu_2 + 2\mu_2) - (j_{11}\nu_1 - j_{12}\nu_2)\right]. \tag{3.13}$$

The intersection of the cores of the $s_k(i_k)$[6] is a (singular in this limit) saddle point. Fig. 1(b) illustrates this situation for $\rho = 1$, $\mu_2 = -.01$, and

$$\tau = \begin{pmatrix} 1 \\ 1 \end{pmatrix}, \quad \nu = \begin{pmatrix} 1 \\ .1 \end{pmatrix}, \quad J = \begin{pmatrix} 1 & .5 \\ .5 & .1 \end{pmatrix}$$

(the choice obeys to the fact that global stability makes condition $j_{21}\nu_1 - j_{22}\nu_2 > -\mu_2$ rather stringent).

[4] With our mind in neurophysiology applications, we shall assume $s_k(i_k)$ to have the same functional form, of sigmoidal shape. But neither condition is necessary to satisfy the integrability condition.

[5] (through an inverse saddle–node bifurcation at the "on" location: in one variable, $\frac{x^2}{2} - a\,(x-a)\,\theta(x-a)$ resets the slope to zero at $x = a$).

[6] (located at the solution $\frac{j_{22}\mu_1 - j_{12}\mu_2}{\det J}, \frac{j_{21}\mu_1 - j_{11}\mu_2}{\det J}$ of $J\mathbf{x} + \mathrm{M} = 0$).

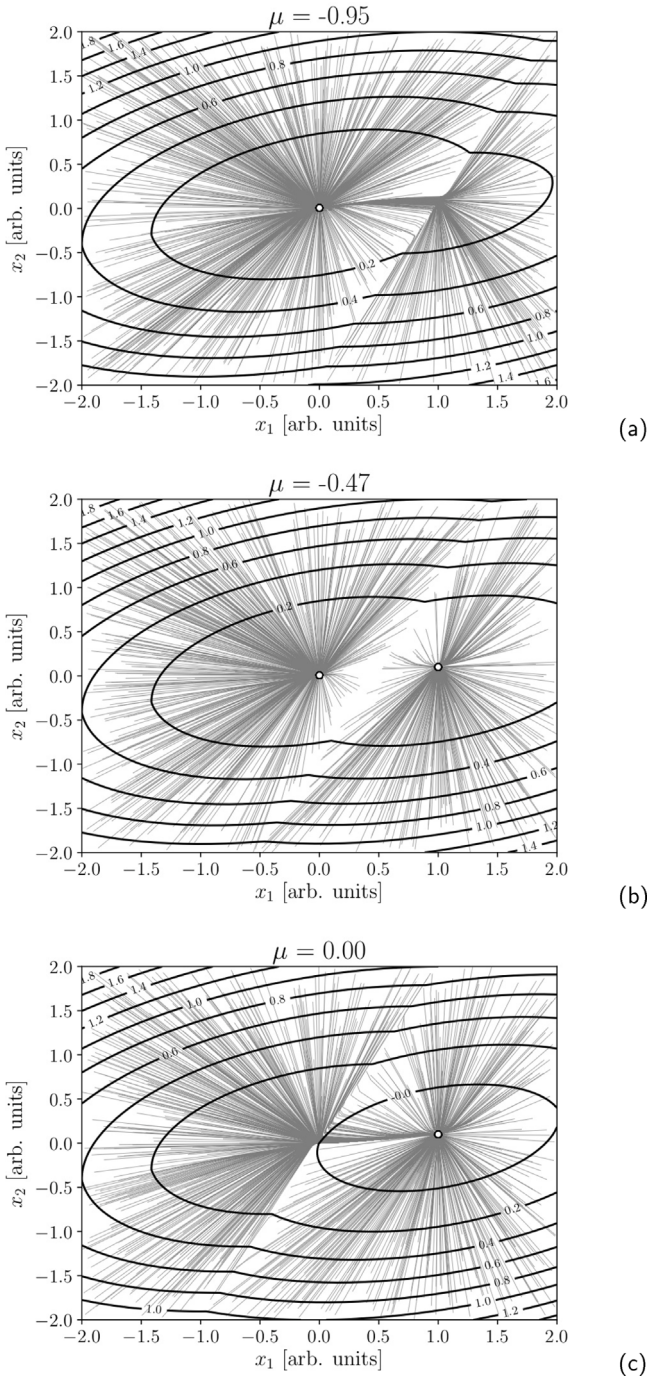

Fig. 1. Illustration of the analytical results in Section 3.2. Trajectories from random initial conditions and contour plot of the NEP—Eq. (3.10), with $S_k(i_k) - S_k(\mu_k)$ given by Eq. (3.12)—in the equistable case given by Eq. (3.13) (b), and near the "off" (a) and "on" (c) saddle–node bifurcations.

- As $\mu_k \to 0$, $k = 1, 2$, this saddle point moves toward the "off" node. After a (direct) saddle–node bifurcation, only the "on" node at $x_k = \nu_k$ remains, since conditions $(J\mathrm{N})_k > -\mu_k$, $k = 1, 2$ are better satisfied, see Fig. 1(c).

The most striking feature of Fig. 1 is the existence of an edge between half planes, whose location translates parallely as μ_1 is varied, from the neighborhood of the "on" node in (a) to that of the "off" one in (c). If there is room for some spreading of the core, the former result remains valid for whatever analytical form of the response functions. In such a case, the saddle point (lying at the crossing of the aforementioned edge with the one joining the nodes) will be analytical.

In the singular limit $s_k(i_k) := \nu_k\, \theta(i_k)$ we deal with in this subsection, we can prove rigorously the nonexistence of limit cycles (at least for large $\mu_k < 0$, $k = 1, 2$). The Bendixson–Dulac theorem states that if there exists a C^1 function $\boldsymbol{\Phi}(\mathbf{x})$ (called the Dulac function) such that $\mathrm{div}(\boldsymbol{\Phi}\mathbf{f})$ has the same sign *almost everywhere*[7] in a simply connected region of the plane, then the plane autonomous system $\dot{\mathbf{x}} = \mathbf{f}(\mathbf{x})$ has no nonconstant periodic solutions lying entirely within the region. Because of Eq. (2.7),

$$\mathrm{div}(\boldsymbol{\Phi}\mathbf{f}) = \mathbf{f}^{\mathrm{T}}(\mathbf{x})\nabla\boldsymbol{\Phi} + \boldsymbol{\Phi}\mathrm{div}\,\mathbf{f} = -(\nabla\boldsymbol{\Phi})^{\mathrm{T}} Q\, \nabla\boldsymbol{\Phi} + \boldsymbol{\Phi}\mathrm{div}\,\mathbf{f}.$$

Clearly, $\mathrm{div}\,\mathbf{f} < 0$ almost everywhere [i.e. except at the cores of the $s_k(i_k)$]. For $\mu_k < 0$ ($k = 1, 2$) and large, $\boldsymbol{\Phi}(\mathbf{x})$ will be essentially the quadratic form in the first term of Eq. (3.10), so it meets the conditions to be a Dulac function in a simply connected region of the plane.

3.2. Extended systems

(a) One-component reaction–diffusion systems

In [2] we have addressed the phenomenon of stochastic resonance in reaction–diffusion systems, exploiting the NEP framework. In particular, we have shown the occurrence of *array-enhanced* and *system-size* stochastic resonance in a scalar (one-component) model with field-dependent diffusion, in both the reaction term and the diffusion coefficient are which piecewise linear, thus allowing for stationary patterns to be found analytically. Among them, one acts as saddle between the "off" and "on" stable patterns, providing a *finite* barrier which depends on the parameters. The phenomena of stochastic resonance and akin occur mainly but *not only* at equistability [53].

(b) Two-component reaction–diffusion systems

Also in [2], the work described in the former paragraph is generalized to a stylized reaction–diffusion version of the FitzHugh–Nagumo system. After an adiabatic-like elimination of the inhibitor field, we derive an effective scalar model that includes a *nonlocal* contribution. Studying the role played by the *range* of the nonlocal kernel and its effect on stochastic resonance, we find an optimal range that maximizes the system's response.

In [75], the nonequilibrium Ising–Bloch front bifurcation of the FitzHugh–Nagumo model with nondiffusing inhibitor provides a beautiful instance of an extended bistable system made up of *propagating* (Bloch) *fronts*. Moreover, these fronts are chiral and parity-related, and the *finite* barrier between them is nonetheless but a stationary Ising front. By means of numerical simulation in the neighborhood of this bifurcation, we demonstrate the existence of stochastic resonance in the transition between Bloch fronts of opposite chiralities, when an additive noise is included. The signal-to-noise ratio is numerically observed to scale with the distance to the critical point. This scaling law is theoretically characterized in terms of an effective NEP.

(c) The complex Ginzburg–Landau equation (CGLE)

This equation is retrieved when z in Eq. (3.4) is let to be a field $z(\mathbf{x})$, $\mathbf{x} \in \mathbb{R}^d$ and a complex diffusion term $d\nabla^2 z$ is added [34]. Eqs. (3.4), (3.6) and (3.7) generalize to

$$\dot{z}(\mathbf{x}) = -\frac{\delta\boldsymbol{\Phi}}{\delta z^*} + r(z(\mathbf{x}), z^*(\mathbf{x})), \tag{3.14}$$

$$\int \mathrm{d}^d x \left[r\,\frac{\delta\boldsymbol{\Phi}}{\delta z} + r^*\frac{\delta\boldsymbol{\Phi}}{\delta z^*}\right] = 0. \tag{3.15}$$

In the supercritical domain $a_1 > 0$, Eq. (3.14) has several further instabilities. Newell and Kuramoto showed that the (arbitrary and spatially constant) phase of z on the extended attractor $|z| = \sqrt{a_1/b_1}$ may become unstable in k–space near $k = 0$, leading to "*phase turbulence*". Moreover, *traveling-wave* attractors which exist in addition to the

[7] Everywhere except possibly in a set of measure 0.

spatially homogeneous one, may become unstable under appropriate conditions, leading to Eckhaus–Benjamin–Feir instability among other phenomena [34].

(d) The KPZ equation

The KPZ equation for kinetic interface roughening (KIR) [76–79],

$$\partial_t h(\mathbf{x},t) = \nu\,\nabla^2 h(\mathbf{x},t) + \frac{\lambda}{2}\,[\nabla h(\mathbf{x},t)]^2 + \xi(\mathbf{x},t), \tag{3.16}$$

where $h(\mathbf{x},t)$ is the interface height and $\xi(\mathbf{x},t)$ a Gaussian noise with

$$\langle \xi(\mathbf{x},t)\rangle = 0\ ,\ \langle \xi(\mathbf{x},t)\xi(\mathbf{x}',t')\rangle = 2D\,\delta^d(\mathbf{x}-\mathbf{x}')\,\delta(t-t'),$$

is nowadays a paradigm of systems exhibiting nonequilibrium critical scaling [80]. In fact—besides standing out as a representative of a large and robust class of microscopic KIR models,[8] from which the phenomenological parameters ν, λ, D can be computed—it is intimately related to the equilibrium statistics of directed polymers and to the Burgers equation of turbulence.

In the literature, it is commonly assumed that the KPZ equation cannot be directly obtained from a Hamiltonian. However, as shown in Ref. [55], there is no trouble in expressing Eq. (3.16) as a stochastic gradient flow,

$$\partial_t h(\mathbf{x},t) = -\frac{\delta \Phi[h]}{\delta h(\mathbf{x},t)} + \xi(\mathbf{x},t).$$

The functional Φ is defined as

$$\Phi[h(\mathbf{x},t)] = \int \mathrm{d}\mathbf{x}\left[\frac{\nu}{2}(\nabla h)^2 - \frac{\lambda}{2}\int_{h_0(\mathbf{x},0)}^{h(\mathbf{x},t)} \mathrm{d}\psi\,(\nabla\psi)^2\right], \tag{3.17}$$

where $h_0(\mathbf{x},0)$ is an *arbitrary* initial pattern (usually assumed to be constant, in particular $h_0 = 0$). The first term is clearly the Landau–Ginzburg free-energy functional

$$\Phi_{\mathrm{EW}}[h(\mathbf{x},t)] = \frac{\nu}{2}\int \mathrm{d}\mathbf{x}\,[\nabla h(\mathbf{x},t)]^2.$$

associated to the (equilibrium) EW process. Unfortunately, the second one has *not* an explicit density. Even though at time t, Φ depends *only* on the field $h(\mathbf{x},t)$, its evaluation requires *knowing the detailed history* that led from h_0 to $h(\mathbf{x},t)$. In other words, retrieving information on Φ (such as its landscape at certain time or the time dependence of its mean value) requires averaging not simply over field configurations $h(\mathbf{x})$ at time t, but over (statistically weighted) *trajectories* of the field configuration.

Being the KPZ equation a (stochastic) gradient one, the functional Φ governing its *deterministic* component provides the *landscape* where the stochastic dynamics of $h(\mathbf{x})$ takes place at time t, and in the absence of noise fulfills explicitly the Lyapunov property $\dot{\Phi}[h] = -\left[\frac{\delta\Phi[h]}{\delta h(x,t)}\right]^2 \le 0$. Unfortunately, this does *not* make Φ into a Lyapunov functional, since (as shown in the next paragraph) it is unbounded from below.

The second term in Eq. (3.17), namely

$$-\frac{\lambda}{2}\int \mathrm{d}\mathbf{x}\int_{h_0(\mathbf{x},0)}^{h(\mathbf{x},t)} \mathrm{d}\psi\,(\nabla\psi)^2,$$

is *not* a functional integral of the form $\int \prod_{\mathbf{x}} \mathrm{d}\psi(\mathbf{x})$ [82,83], but a kind of "grand mean" of $(\nabla h)^2$. For a suitably small time τ, the integral over ψ at fixed $\mathbf{x}$ can be evaluated by resort to the Mean Value Theorem, yielding

$$\int_{h_0(\mathbf{x},0)}^{h(\mathbf{x},\tau)} \mathrm{d}\psi\,(\nabla\psi)^2 \approx [h(\mathbf{x},\tau) - h(\mathbf{x},0)]\left[\nabla\tilde{h}(\mathbf{x})\right]^2,$$

[8] We deliberately leave aside KIR models exhibiting diverse kinds of *anomalous* scaling [3,81].

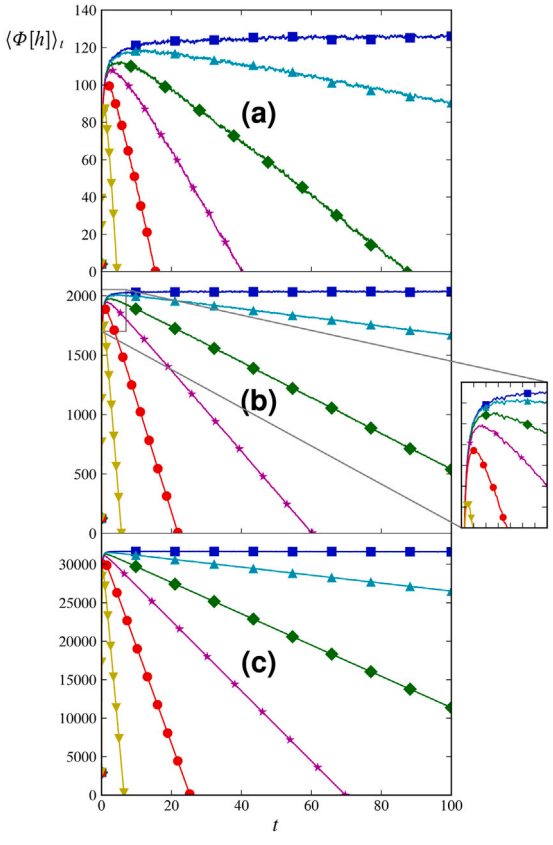

Fig. 2. Time behavior of $\Phi[h]$, averaged over 100 samples, in (a) 1d (size 1024), (b) 2d (size 128^2), and (c) 3d (size 64^3). The symbols (denoting a subset of the simulation points) indicate the values adopted for λ in each curve. ■ : $\lambda = 0.01$, ▲ : $\lambda = 0.10$, ⋄ : $\lambda = 0.20$, ★ : $\lambda = 0.30$, • : $\lambda = 0.50$, ▼ : $\lambda = 1.00$. Inset: Detail showing the existence of maxima in 2d for *any* $\lambda > 0$ (the same occurs in 1d and 3d).

where $\tilde{h}(\mathbf{x})$ is some intermediate value between $h(\mathbf{x},\tau)$ and $h(\mathbf{x},0)$. For finite time t, a discretization with step τ and index μ yields

$$\begin{aligned}\int_{h_0(\mathbf{x},0)}^{h(\mathbf{x},t)} \mathrm{d}\psi\,(\nabla\psi)^2 &\approx \sum_{\mu=0}^{M-1} \tau\,\frac{h_{\mu+1}(\mathbf{x}) - h_\mu(\mathbf{x})}{\tau}\left[\nabla\tilde{h}_\mu(\mathbf{x})\right]^2 \\ &\approx \int_0^t \mathrm{d}s\,\dot{h}(\mathbf{x},s)[\nabla h(\mathbf{x},s)]^2,\end{aligned}$$

with $\tilde{h}_\mu(\mathbf{x})$ intermediate between $h_\mu(\mathbf{x})$ and $h_{\mu+1}(\mathbf{x})$, and $\dot{h}(\mathbf{x},s) := \lim_{\tau\to 0}[h_{\mu+1}(\mathbf{x}) - h_\mu(\mathbf{x})]/\tau$. This allows us to write the potential in the form

$$\Phi[h] = \int \mathrm{d}\mathbf{x}\left\{\frac{\nu}{2}(\nabla h)^2 - \frac{\lambda}{2}\int_0^t \mathrm{d}s\,\dot{h}(\mathbf{x},s)[\nabla h(\mathbf{x},s)]^2\right\}, \tag{3.18}$$

which highlights the fact that even though the field $h(\mathbf{x},t)$ obeys a Fokker–Planck equation (thus it is Markovian, albeit without stationary regime), it evolves at every time in an adaptive potential landscape, which itself evolves according to the *whole* history of $h(\mathbf{x},t)$ and has thus a very long ("infinite") memory [61]. The dependence of the asymptotic statistics in 1D [84–88] on the topology of the substrate might probably be traced back to this fact.

Spectral methods pay back the overhead of Fourier transforming $h(\mathbf{x})$ forth and back every time t, with a discrete approximation of ∇h of the order of the system's size. They have proved to be more stable and reliable than pure real-space finite-differences schemes in the integration of some nonlinear growth equations [89–91]. Using a spectral method to integrate Eq. (3.16), we have analyzed the time behavior of $\langle\Phi[h]\rangle_t$ (the average of Φ over noise realizations, at time t) as given by Eq. (3.18).

Fig. 2 displays the time dependence of the NEP's average over 100 samples, for systems in 1d (size 1024), 2d (size 128^2), and 3d (size 64^3), and several values of λ, starting from flat initial conditions. For *any* $\lambda > 0$ there is a maximum, where the nonlinear (KPZ) term overcomes the linear (EW) one.[9] Hence we see two evident advantages of the NEP in KPZ: its maximum gives a visual criterion for the EW–KPZ crossover and its linearly decreasing range (whose slope goes as λ^2) does the same for the KPZ scaling regime. Among other issues discussed in [61] are the similarity of the KPZ process with an escape one, and the relationship between the asymptotic form of the NEP and the asymptotic front speed v_∞.

Before leaving this section, it is worth noting the interesting work of Harris and Ermentrout [92] on traveling waves in the Wilson-Cowan model. Although the system is potential only when the ranks of the interaction kernels are equal, such a case is representative of generic behavior.

4. Applications in stochastic thermodynamics

For nearly a century or more, the only consistent framework to tackle scientific and technological problems was equilibrium thermodynamics which as known, is based on two postulates: equilibrium and the so-called "thermodynamic limit". Like sailors before Columbus, for nearly an additional half a century, our most daring detachment from equilibrium was weak disequilibrium, whose most celebrated result is Onsager's reciprocal relations [3]. Even within that limited scope, a key concept for further development was identified: *entropy production*.

Today, we could not be doing nanotechnology and molecular biophysics if it were not for the development in the last two decades of stochastic thermodynamics (ST). Since it is not our purpose here to describe this development, we refer to a few arbitrarily chosen reviews [93–96] and focus on two specific topics, the Jarzynski equality and thermodynamic uncertainty relations (TUR), from the viewpoint of the NEP.

4.1. Jarzynski equality in the Wilson–Cowan model

Far from the thermodynamic limit, thermodynamics' "second law" becomes true only in probability. Early in the development of ST, a number of "fluctuation theorems" encoded this result, one of the most known being the Jarzynski equality for general processes beginning and ending at equilibrium [64,97]: It relates the average of the irreversible work done along an ensemble of trajectories joining the same equilibrium states with the difference between their free energies,

$$\langle \exp(-W/kT)\rangle = \exp(-\Delta F/kT),$$

which can be recast as

$$\langle \exp[(W-\Delta F)/kT)\rangle = 1. \tag{4.1}$$

As argued in [98] for nonequilibrium steady states (NESS)—and further generalized in [99] to *arbitrary* nonequilibrium states—we wish next to obtain some transient fluctuation theorems for $Y^{\rm F} := \int {\rm d}t\, \dot\mu\, \frac{\partial \Phi}{\partial \mu}$, when some control parameter μ on which $V(x_1)$ depends is externally varied according to some protocol $\mu(t)$. From Eq. (?),

$$Y^{\rm F} = \frac{1}{\gamma D}\int {\rm d}t\, \dot\mu^{\rm F}\, \frac{\partial V}{\partial \mu}, \quad Y^{\rm B} = \frac{1}{\gamma D}\int {\rm d}t\, \dot\mu^{\rm B}\, \frac{\partial V}{\partial \mu}. \tag{4.2}$$

If μ is varied linearly from $-\tau$ to τ, then $\dot\mu^{\rm B} = -\dot\mu^{\rm F} = {\rm const}$, and $Y^{\rm B} = -Y^{\rm F}$ along each trajectory. For the undriven Duffing oscillator we may take $\mu := \omega_0^2$, imagining the oscillator is realized as a Moon beam, and the magnets are moved steadily in such a way that the pitchfork bifurcation is come across. If ω_0^2 goes from 1 to -1 in 2τ,

$$Y^{\rm F} = -\frac{1}{2\gamma D\tau}\int_{-\tau}^{+\tau} {\rm d}t\, x_1^2(t).$$

According to [98], when both protocol and dynamics are jointly reversed, the distributions $\rho(y)$ of Y–values in an ensemble of realizations of the respective processes (keeping the endpoints fixed) obey

$$\frac{\rho^{\rm F}(y)}{\hat\rho^{\rm B}(-y)} = \exp(y), \tag{4.3}$$

where in $\hat\rho^{\rm B}$, $x_2 \to -x_2$. Eq. (4.3) has a Jarzynski-like integrated version

$$\langle \exp(-y)\rangle^{\rm F} = 1, \tag{4.4}$$

where $\langle\bullet\rangle^{\rm F}$ denotes average over realizations of the forward process. From [98],

$$\rho^{\rm F}(y) = \int_{x_1(t_i)=x_1^i}^{x_1(t_f)=x_1^f} \mathcal{D}[x_1] {\rm e}^{S_3(D)^{\rm F}}\, \delta(Y^{\rm F}-y)$$

$$\hat\rho^{\rm B}(-y) = \int_{x_1(t_i)=x_1^i}^{x_1(t_f)=x_1^f} \mathcal{D}[x_1] {\rm e}^{S_3(D)^{\rm B}}\, \delta(Y^{\rm B}+y)$$

We may reason trajectorywise with the aid of the canonical momenta $p_Y^{\rm F}$, $p_Y^{\rm B}$ conjugated to $Y^{\rm F}$ and $Y^{\rm B}$.

In order to generate such an ensemble, we start from the trajectory in Fig. 2 and introduce random deviations with variance D along it.

4.2. Thermodynamic uncertainty relation in KPZ [62]

As found in [65], the entropy production rate σ in a nonequilibrium steady state (NESS) turns out to be bounded from below by the ratio between the squared mean and the variance of an arbitrary current.[10] This result was followed by several others [100–104], known generically as "thermodynamic uncertainty relations" (TUR). Recently, a TUR has been discussed for KPZ [105–107].

In [108], the TUR were shown to stem from the Cramer–Rao inequality [109]: for a multivariate generalized (or "multiplicative") Langevin equation

$$\dot{\mathbf{x}} = \mathbf{A}_\theta(\mathbf{x},t) + \sqrt{2}\mathbf{C}(\mathbf{x},t)\,\Xi(t),$$

depending on a real parameter θ.

Following [108], we now derive another TUR. We start by adding to Eq. (3.16) a constant F, representing, e.g. a particle flux in molecular-beam epitaxy (MBE).

We can relate our equation (KPZ) with the equations in [108] (i.e. Eq. (1)). The spatial variable could be in any dimension, that is

- $x_i = h_i(r,t)$
- $\theta = F$
- $A_\theta|_i = (\nu\nabla^2 h(\bar r,t) + \frac{\lambda}{2}(\nabla h(\bar r,t))^2 + F)|_i$
- $\sqrt{2}C(\mathbf{x},t) = 1$
- B is a diagonal matrix with elements $\epsilon/2$
- etc ...

For the "estimator" $\Theta[\Gamma]$ (Γ a trajectory), we adopt the entropy production $\Theta[\Gamma] = R^F(h_a,h_b)$ (to start, at $t=0$ we assume flat initial conditions, but it is easy to generalize for arbitrary initial conditions). Hence, in what follows, $\Phi[h_a]=0$. Then we have

$$R^F(h_a,h_b) = -\big(\Phi[h_b]-\Phi[h_a]\big) = -\Phi[h_b]. \tag{4.5}$$

We shall not repeat here all the steps done in the indicated reference, but it is worth indicating the use of a vector notation (in particular in 1d, but that could be extended to any dimension).

[9] Only for $\lambda = 0$ (corresponding to EW) is there true saturation. The $\lambda = 0.01$ case shown here (visually resembling a saturation behavior) attains its maximum outside the plotted range.

[10] Specifically, after a time t in the NESS, a fluctuating integrated current $X(t)$ has a mean $\langle X(t)\rangle = jt$, and a diffusivity $D = (2t)^{-1}\lim_{t\to\infty}\langle (X(t)-jt)^2\rangle$. Then $\sigma \geq j^2/2D$.

In order to simplify, we define

- $\frac{\nu}{2}(h_{j+1}+h_{j-1}-2h_j) \equiv \left(\nu\nabla^2 h\right)|_j$
- $\frac{\lambda}{2}\left(\frac{((h_{j+1}-h_j)^2+(h_j-h_{j-1})^2)}{2}\right) = \left(\frac{\lambda}{2}\left(\nabla h(\bar{r},t)\right)^2\right)|_j$

as with this definitions, as used in the NEP, we get a discrete representation [56–59] that, if not "exact" at least is *coherent*.

We exploit the "Cramer–Rao inequality" (as described in [108]). Hence, we have the relation

$$\frac{var(\Theta[\Gamma])}{(\partial_F\langle\Theta[\Gamma]\rangle)^2_F} \geq (I(\Gamma))^{-1} \tag{4.6}$$

with $I(\Gamma)$ the Fisher information. It is given by

$$I(\Gamma) = \langle\left(\partial_F \ln P_F(\Gamma)\right)^2\rangle_F = -\langle\partial_F^2 \ln P_F(\Gamma)\rangle_F.$$

Using the definition of mean values along trajectories Γ, that is $\langle\Theta(\Gamma)\rangle|_F$, etc. And with a flat initial condition, we get

$$I(F) = \frac{1}{2\varepsilon}\langle T\Omega\rangle_F = \frac{T\Omega}{2\varepsilon}, \tag{4.7}$$

where Ω is the volume in dimension d. We used that

$$\partial_F A_{j,F} = 1.$$

With a non flat initial condition, with the approximate pdf

$$\hat{P}(h_f, t_f) \approx e^{-S_0[h_f,t_f]/\varepsilon},$$

we get

$$I(F) \sim \frac{T\Omega}{2\varepsilon}.$$

Hence, the form of the TUR is

$$\frac{\langle(R^F(h^F) - \langle R^F(h^F)\rangle_F)^2\rangle_F}{(\partial_F\langle R^F(h^F)\rangle)^2} \geq \frac{2\varepsilon}{T\Omega}. \tag{4.8}$$

Eventually, we could make all the evaluation more precise, exploiting that, asymptotically, $h(r,t) \approx v_\infty t + (\Gamma t)^\beta \chi(r')$, with $r' = (Ar/2)(\Gamma t)^{-1/z}$, $A = \nu/2\varepsilon$, $\Gamma = A^2\lambda/2$ ($\beta = 1/3$, $z = 3/2$, $\alpha = 1/2$).

5. Other applications

5.1. System-size stochastic resonance in Wilson–Cowan

The adaptability of the neocortex to changing environments shows its high susceptibility, a property of critical systems. As there is no fine tuning, self-organized criticality [110] or Griffiths phases [111] have been thought of. Another possibility is stochastic resonance, since the Wilson–Cowan model presents a bistable regime. But also, as this is a population model, it can show system-size stochastic resonance.

If we set the external input μ_1 to μ_{1b} and add a small harmonic signal to it, so that $\mu_1 = \mu_{1b} + \Delta\mu_1\cos(\omega t)$, with $1/\omega \gg \max(\tau_1, \tau_2)$ we are able to study the stochastic resonance. Since the signal is slow, we can consider that the NEP adapts to the instantaneous value of μ_1 (adiabatic approximation) and the frequencies are those corresponding to the value of μ_1 "given by Fig. 1". To calculate the signal-to-noise ratio R, as usual, we linearize the values of ω_k around $\mu_1 = \mu_{1b}$. The values of the coordinates of the critical points for μ_{1b} are: $\mathbf{x}^{*1} = (0, 0.1)^T$, $\mathbf{x}^{*2} = (1, 0.99)^T$ and $\mathbf{x}^* = (0.5, 0.58)^T$. The values of the Hessian determinants are $\mathrm{H}(\Phi(\mathbf{x}^{*1})) = 1.93$, $\mathrm{H}(\Phi(\mathbf{x}^{*2})) = 0.84$ and $\mathrm{H}(\Phi(\mathbf{x}^*)) = -15.73$ and the positive eigenvalue of the Jacobian in the saddle is $\lambda_+^* = 4.84$, all in $\mu_1 = \mu_{1b}$. The common value of both barriers without signal is $\Delta\Phi_0 = 0.12$. Neglecting terms $\mathcal{O}(\Delta\mu)^2$, the linearized escape frequencies remain, as

$$\omega_1 = \omega_{10} - \alpha_{10}\Delta\mu_1\cos(\omega t) \tag{5.1}$$

$$\omega_2 = \omega_{20} + \alpha_{20}\Delta\mu_1\cos(\omega t) \tag{5.2}$$

$$\omega_{10} = 0.27\exp(-0.12/D) \tag{5.3}$$

$$\omega_{20} = 0.18\exp(-0.12/D) \tag{5.4}$$

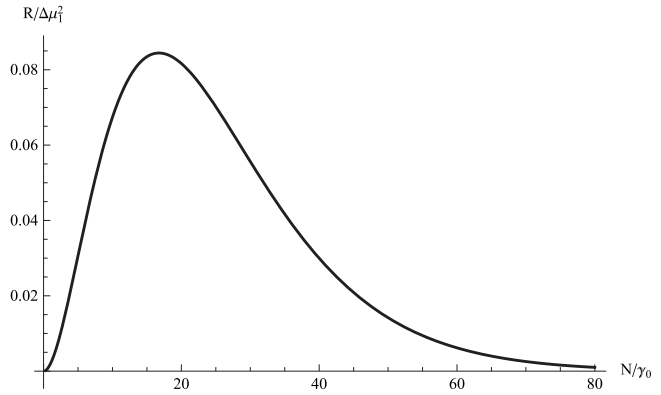

Fig. 3. Signal-to-noise ratio for $\tau_1 = \tau_2 = \rho = \nu_1 = \nu_2 = \beta_2 = 1$, $\beta_1 = 1.2$, $\mu_1 = -3.723$, $\mu_2 = 0$, $j_{11} = 12$, $j_{12} = 4$, $j_{21} = 13$, $j_{22} = 11$. The maximum $R_{\max} = 8.44\times10^{-2}\Delta\mu_1^2$ is attained for $N = 17D_0$.

$$\alpha_{10} = (0.022/D)\exp(-0.12/D) \tag{5.5}$$

$$\alpha_{20} = (0.014/D)\exp(-0.12/D). \tag{5.6}$$

Finally, the signal-to-noise ratio R [53] is given by

$$R = \frac{\pi(\Delta\mu_1)^2(\alpha_{20}\omega_{10} + \alpha_{10}\omega_{20})^2}{4\omega_{10}\omega_{20}(\omega_{10}+\omega_{20})} + \mathcal{O}(\Delta\mu_1)^4. \tag{5.7}$$

Taking into account the relation between the intensity of the noise and the size of the system [112] given by $D = D_0/N$, with D_0 independent of N, we see that the model presents SSSR, as shown in Fig. 3, where we plot the signal-to-noise ratio as a function of the size of the system, that is, the number N of neurons. Since $R \sim \exp(-\Delta\Phi_0/D)/D^2$, the maximum of R is at $N = 2D_0/\Delta\Phi$ ($D = \Delta\Phi/2$).

5.2. Memory of initial conditions in KPZ

The simulations in Section 3.2 have been performed starting from flat initial conditions (IC). Given that (a) in 1D, the topology of the IC determines the front's statistics in the scaling regime and (b) the NEP keeps memory of the whole process [61], it is interesting to see how the results in Fig. 2 change when other IC are considered. Fig. 4 shows simulations by spectral methods in the same conditions as in Fig. 2 (100 realizations, up to $t = 100$ with $\epsilon = 0.5$ and $\nu = 1$) but for a single value of $\lambda = 0.1$ in 1D and 2D.

In 1D, the initial condition is a function of the form

$$\mathrm{abs}(x - L/2)/a, \quad a \in \{0.5, 1.5, 3, 20\}.$$

The flat-surface initial condition is also included. The system size is $L = 1024$. The light blue curve corresponds to $a = 0.5$ and the dark blue one to $a = 20$. In the studied time interval, the slopes depend strongly on the IC.

In 2D, the initial condition is of the pyramidal type with vertex at $(L/2, L/2)$ and value $L/(2a)$ at the edges of the system. The values of a are in this case $\{0.75, 1, 1.5, 3, 20\}$. The flat-surface initial condition is also included. The system size is $L \times L$, with $L = 128$. The light blue curve corresponds to $a = 0.55$ and the dark blue one to $a = 20$. In the studied time interval, not only do the slopes depend strongly on the IC but a concavity is observed in some curves.

These preliminary results tell us that there is an optimal population size that gives maximum susceptibility. .

6. Conclusions

The fact that every Langevin system whose Fokker–Planck equation admits a stationary solution is a potential one is not a minor issue, as neither is the fact that by means of noise, one can eventually condition a nonpotential deterministic system to become a potential one.

We have introduced two new instances of potential systems:

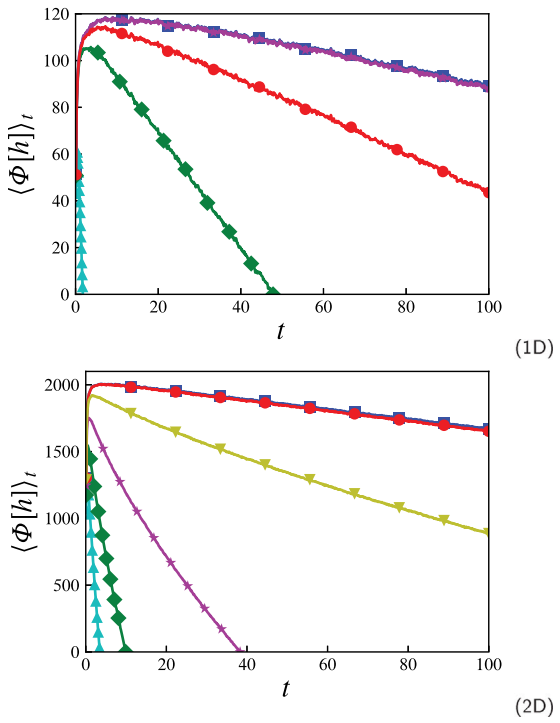

Fig. 4. Ensemble average of $\Phi[h]$ in Eq. (3.18), for $\lambda = 0.1$. (1D): $a = 0.5$ (light blue), 1.5 (dark green), 3 (red), 20 (dark blue), and ∞ (magenta). (2D) $a = 0.75$ (light blue), 1.0 (green), 1.5 (magenta), 3 (light green), 20 (dark blue), and ∞ (red). (For interpretation of the references to color in this figure legend, the reader is referred to the web version of this article.)

a. The celebrated KPZ equation—the stochastic field theory of kinetic roughening—turned out to be a (stochastic) gradient flow in a self-consistent, adaptive landscape [55]. Among the virtues of the functional it stems from, yielding visual criteria for the EW–KPZ crossover and the onset of the scaling regime can be remarked [61].
b. The Wilson–Cowan rate model of the neocortex is generically a non-relaxational potential system for vanishing refractory times. The facts that it becomes relaxational for equal relaxation times and that it cannot sustain limit cycles for vanishing refractory times can also be remarked [63].

The usefulness of the NEP for obtaining results in stochastic thermodynamics has been illustrated by deriving a Jarzynski equality in the equal-relaxation-times Wilson–Cowan model and a novel thermodynamic uncertainty relation (TUR) in the KPZ equation.

That the NEP is useful to obtain results in phenomena akin to stochastic resonance is not a novelty. Here we illustrate this fact by showing the existence of system-size stochastic resonance in the Wilson Cowan model, exploiting the fact that it is itself a population model.

Finally, we advance preliminary results on the dependence of the ensemble average of the KPZ NEP on initial conditions, a subject that deserves further study.

Data availability

No data was used for the research described in the article.

Acknowledgment

H.S.W. and R.R.D. thank warmly M. A. Rodríguez and R. Toral for enlightening discussions on the subject of this work, sustained along more than three decades. A.D.S. and R.R.D. acknowledge support by UNMdP, Argentina through project EXA1033/21–15/E991.

References

[1] Wio HS. Nonequilibrium potential in reaction–diffusion systems. In: Garrido P, Marro J, editors. 4th granada seminar in computational physics. Dordrecht: Springer; 1997, p. 135–95.
[2] Wio HS, Deza RR. Aspects of stochastic resonance in reaction–diffusion systems: The nonequilibrium-potential approach. Eur Phys J Spec Top 2007;146:111–26.
[3] Wio HS, Deza RR, López JM. An introduction to stochastic processes and nonequilibrium statistical physics, revised edition. Singapore: World Scientific; 2012.
[4] Kirkpatrick S, Gelatt CD, Vecchi MP. Optimization by simulated annealing. Science 1983;220:671–80.
[5] Yan H, Zhao L, Hu L, Wang X, Wang E, Wang J. Nonequilibrium landscape theory of neural networks. Proc Nat Acad Sci USA 2013;110:E4185–94.
[6] Wang J, Oliveira RJ, Chu X, Whitford PC, Chahine J, Han W, Wang E, Onuchic JN, Leite VB. Topography of funneled landscapes determines the thermodynamics and kinetics of protein folding. Proc Nat Acad Sci USA 2012;109:15763–8.
[7] Wang J, Huang B, Xia X, Sun Z. Funneled landscape leads to robustness of cell networks: Yeast cell cycle. PLoS Comput Biol 2006;2:e147.
[8] Kim K-Y, Wang J. Potential energy landscape and robustness of a gene regulatory network: Toggle switch. PLoS Comput Biol 2007;3:60.
[9] Wang J, Xu L, Wang E, Huang S. The potential landscape of genetic circuits imposes the arrow of time in stem cell differentiation. Biophys J 2010;99:29–39.
[10] Li C, Wang E, Wang J. Potential landscape and probabilistic flux of a predator prey network. PLoS Comput Biol 2011;6:e17888.
[11] Zhang F, Xu L, Zhang K, Wang E, Wang J. The potential and flux landscape theory of evolution. J Chem Phys 2012;137:065102.
[12] San Miguel M, Toral R. Stochastic effects in physical systems. In: Tirapegui E, Martínez-Mardones J, Tiemann R, editors. Instabilities and nonequilibrium structures VI. Dordrecht: Springer; 2000, p. 35–127.
[13] Montagne R, Hernández-Garcí E, San Miguel M. Numerical study of a Lyapunov functional for the complex Ginzburg–landau equation. Physica D 1996;96:47–65.
[14] Graham R, Haken H. Generalized thermodynamic potential for Markoff systems in detailed balance and far from thermal equilibrium. Z Phys 1971;243:289–302.
[15] Graham R. Generalized thermodynamic potential for the convection instability. Phys Rev Lett 1973;31:1479.
[16] Graham R. Hydrodynamic fluctuations near the convection instability. Phys Rev A 1974;10:1762.
[17] Swift J, Hohenberg PC. Hydrodynamic fluctuations at the convective instability. Phys Rev A 1977;15:319.
[18] Grabert H, Green MS. Fluctuations and nonlinear irreversible processes. Phys Rev A 1979;19:1747.
[19] Grabert H, Graham R, Green MS. Fluctuations and nonlinear irreversible processes. II. Phys Rev A 1980;21:2136.
[20] Graham R, Tél T. Existence of a potential for dissipative dynamical systems. Phys Rev Lett 1984a;52:9.
[21] Graham R, Tél T. On the weak-noise limit of fokker–Planck models. J Stat Phys 1984b;35:729–49.
[22] Graham R, Roekaerts D, Tél T. Integrability of hamiltonians associated with fokker–Planck equations. Phys Rev A 1985;31:3364.
[23] Graham R, Tél T. Weak-noise limit of Fokker–Planck models and non-differentiable potentials for dissipative dynamical systems. Phys Rev A 1985;31:1109.
[24] Graham R. Weak noise limit and nonequilibrium potentials of dissipative dynamical systems. INS 1985;1:271.
[25] Graham R, Tél T. Nonequilibrium potential for coexisting attractors. Phys Rev A 1986;33:1322.
[26] Graham R, Tél T. Nonequilibrium potentials for local codimension-2 bifurcations of dissipative flows. Phys Rev A 1987;35:1328.
[27] Graham R. Weak noise limit and nonequilibrium potentials of dissipative dynamical systems. In: Tirapegui E, Villarroel D, editors. Instabilities and nonequilibrium structures. Dordrecht: Reidel; 1987, p. 271–90.
[28] Graham R, Tél T. Erratum: Nonequilibrium potential for coexisting attractors. Phys Rev A 1988;38:5944.
[29] Tél T, Graham R, Hu G. Nonequilibrium potentials and their power-series expansions. Phys Rev A 1989;40:4065.
[30] Graham R. Macroscopic potentials, bifurcations and noise in dissipative systems. In: Moss F, McClintock PVE, editors. Noise in nonlinear dynamical systems, v.1. CUP; 1989, p. 225–78.
[31] Graham R, Hamm A, Tél T. Nonequilibrium potentials for dynamical systems with fractal attractors or repellers. Phys Rev Lett 1991;66:3089.
[32] Bertini L, De Sole A, Gabrielli D, Jona-Lasinio G, Landim C. Fluctuations in stationary nonequilibrium states of irreversible processes. Phys Rev Lett 2001;87:040601.
[33] Descalzi O, Martínez S, Tirapegui E. Thermodynamic potentials for non-equilibrium systems. Ch Sol Fract 2001;12:2619–30.

[34] Graham R, Tél T. Steady-state ensemble for the complex Ginzburg–landau equation with weak noise. Phys Rev A 1990;42:4661.
[35] Descalzi O, Graham R. Gradient expansion of the nonequilibrium potential for the supercritical Ginzburg–Landau equation. Phys Lett A 1992;170:84–90.
[36] Descalzi O, Graham R. Nonequilibrium potential for the Ginzburg–Landau equation in the phase-turbulent regime. Z Phys B 1994;93:509–13.
[37] Montagne R, Hernández-Garcí E, San Miguel M. Winding number instability in the phase-turbulence regime of the complex Ginzburg–Landau equation. Phys Rev Lett 1996;77:267–70.
[38] San Miguel M, Montagne R, Amengual A, Hernández-Garcí E. Multiple front propagation in a potential non-gradient system. IWINSV 9502003, 1996, p. 85–97.
[39] Montagne R, Hernández-Garcí E, Amengual A, San Miguel M. Wound-up phase turbulence in the complex Ginzburg–Landau equation. Phys Rev E 1997;56:151.
[40] Montagne R, Colet P. Nonlinear diffusion control of spatiotemporal chaos in the complex Ginzburg–Landau equation. Phys Rev E 1997;56:4017.
[41] Izús GG, Deza RR, Wio HS. Exact nonequilibrium potential for the FitzHugh–Nagumo model in the excitable and bistable regimes. Phys Rev E 1998;58:93–8.
[42] Izús GG, Deza RR, Wio HS. Critical slowing-down in the FitzHugh–Nagumo model: A non-equilibrium potential approach. Comput Phys Comm 1999;121–122:406–7.
[43] Izús GG, Sánchez AD, Deza RR. Noise-driven synchronization of a FitzHugh–Nagumo ring with phase-repulsive coupling: A perspective from the system's nonequilibrium potential. Physica A 2009;388:967–76.
[44] Sánchez AD, Izús GG. Nonequilibrium potential for arbitrary-connected networks of FitzHugh–Nagumo elements. Physica A 2010;389:1931–44.
[45] Sánchez A, Izús G, dell'Erba M, Deza R. A reduced gradient description of stochastic-resonant spatiotemporal patterns in a FitzHugh–Nagumo ring with electric inhibitory coupling. Phys Lett A 2014;378:1579–83.
[46] Sánchez A, Izús G, dell'Erba M, Deza R. Hub-enhanced noise-sustained synchronization of an externally forced FitzHugh–Nagumo ring. Physica A 2017;468:289–98.
[47] Wio HS. Stochastic resonance in a spatially extended system. Phys Rev E 1996;54:3075R.
[48] Zanette DH, Wio HS, Deza R. Nonequilibrium potential for a reaction–diffusion model: Critical behavior and decay of extended metastable states. Phys Rev E 1996;53:353.
[49] Drazer G, Wio HS. Nonequilibrium potential approach: Local and global stability of stationary patterns in an activator-inhibitor system with fast inhibition. Physica A 1997;240:571–85.
[50] Kuperman MN, Wio HS, Izús G, Deza R. Stochastic resonant media: Signal-to-noise ratio for the activator-inhibitor system through a quasivariational approach. Phys Rev E 1998;57:5122.
[51] Castelpoggi F, Wio HS. Stochastic resonant media: Effect of local and nonlocal coupling in reaction–diffusion models. Phys Rev E 1998;57:5112.
[52] Bouzat HS, Wio S. Nonequilibrium potential and pattern formation in a three-component reaction–diffusion system. Phys Lett A 1998;247:297–302.
[53] Bouzat S, Wio HS. Stochastic resonance in extended bistable systems: The role of potential symmetry. Phys Rev E 1999;59:5142.
[54] von Haeften B, Deza R, Wio HS. Enhancement of stochastic resonance in distributed systems due to a selective coupling. Phys Rev Lett 2000;84:404.
[55] Wio HS. Variational formulation for the KPZ and related kinetic equations. Int J Bifurcation Chaos 2009;19:2813.
[56] Wio HS, Revelli JA, Deza RR, Escudero C, de La Lama MS. KPZ equation: Galilean-invariance violation, consistency, and fluctuation–dissipation issues in real-space discretization. Europhys Lett 2010a;89(1–6):40008.
[57] Wio HS, Revelli JA, Deza RR, Escudero C, de La Lama MS. Discretization-related issues in the Kardar–Parisi–Zhang equation: Consistency, Galilean-invariance violation, and fluctuation–dissipation relation. Phys Rev E 2010b;81(1–11):066706.
[58] Wio HS, Escudero C, Revelli JA, Deza RR, de La Lama MS. Recent developments on the Kardar–Parisi–Zhang surface-growth equation. Phil Trans R Soc A 2011;369:396–411.
[59] Wio HS, Deza RR, Escudero C, Revelli JA. Invited review: KPZ. recent developments via a variational formulation. Pap Phys 2013a;5:050010.
[60] Wio HS, Deza RR, Revelli JA, Escudero C. A novel approach to the KPZ dynamics. Acta Phys Polon B 2013b;44:889–98.
[61] Wio HS, Rodríguez MA, Gallego R, Revelli JA, Alés A, Deza RR. d–dimensional KPZ equation as a stochastic gradient flow in an evolving landscape: Interpretation, parameter dependence, and asymptotic form. Front Phys 2017;4:52.
[62] Wio HS, Rodríguez MA, Gallego R. Variational approach to KPZ: Fluctuation theorems and large deviation function for entropy production. Chaos 2020;30:073107.
[63] Deza RR, Deza JI, Martínez N, Mejías JF, Wio HS. A nonequilibrium-potential approach to competition in neural populations. Front Phys 2019;6:154.
[64] Jarzynski C. Nonequilibrium equality for free energy differences. Phys Rev Lett 1997;78:2690.
[65] Barato AC, Seifert U. Thermodynamic uncertainty relation for biomolecular processes. Phys Rev Lett 2015;114:158101.
[66] von Haeften B, Izús GG, Wio HS. System size stochastic resonance: General nonequilibrium potential framework. Phys Rev E 2005;72:021101.
[67] Doob JL. Stochastic processes. New York: Wiley; 1953.
[68] Toral R, Colet P. Stochastic numerical methods: An introduction for students and scientists. Weinheim: Wiley-VCH; 2014.
[69] Novikov EA. Functionals and the random-force method in turbulence theory. Sov Phys—JETP 1965;20:1290–4.
[70] Hodgkin AL, Huxley AF. A quantitative description of membrane current and its application to conduction and excitation in nerve. J Physiol 1952;117:500–44.
[71] FitzHugh R. Mathematical models of threshold phenomena in the nerve membrane. Bull Math Biophys 1955;17:257–78.
[72] Nagumo J, Arimoto S, Yoshizawa S. An active pulse transmission line simulating nerve axon. Proc IRE 1962;50:2061–70.
[73] Wilson HR, Cowan JD. Excitatory and inhibitory interactions in localized populations of model neurons. Biophys J 1972;12:1–24.
[74] Borisyuk RM, Kirillov AB. Bifurcation analysis of a neural network model. Biol Cybernet 1992;66:319–25.
[75] dell'Erba MG, Izús GG, Wio HS, Deza RR. Stochastic resonance between counterpropagating Bloch walls: A nonequilibrium-potential description in a neighborhood of the nonequilibrium Ising–Bloch bifurcation. Eur Phys J D 2011;62:103–8.
[76] Kardar M, Parisi G, Zhang Y-C. Dynamic scaling of growing interfaces. Phys Rev Lett 1986;56:889–92.
[77] Halpin-Healy T, Zhang Y-C. Kinetic roughening phenomena, stochastic growth, directed polymers and all that: Aspects of multidisciplinary statistical mechanics. Phys Rep 1995;254:215–414.
[78] Barabási A-L, Stanley HE. Fractal concepts in surface growth. Cambridge, UK: Cambridge U. Press; 1995.
[79] Krug J. Origins of scale invariance in growth processes. Adv Phys 1997;46:139–282.
[80] Lesne A, Laguës M. Scale invariance: from phase transitions to turbulence. Berlin: Springer; 2012.
[81] Ramasco JJ, López JM, Rodrí MA. Generic dynamic scaling in kinetic roughening. Phys Rev Lett 2000;84:2199–202.
[82] Langouche F, Roekaerts D, Tirapegui E. Functional integration and semiclassical expansions. Dordrecht: Reidel; 1982.
[83] Wio HS. Path integrals for stochastic processes: An introduction. Singapore: World Scientific; 2013.
[84] Prähofer M, Spohn H. Statistical self-similarity of one-dimensional growth processes. Physica A 2000a;279:342–52.
[85] Prähofer M, Spohn H. Universal distributions for growth processes in 1+1 dimensions and random matrices. Phys Rev Lett 2000b;84:4882–5.
[86] Sasamoto T, Spohn H. One-dimensional Kardar–Parisi–Zhang equation: An exact solution and its universality. Phys Rev Lett 2010;104(1–4):230602.
[87] Calabrese P, Le Doussal P. Exact solution for the Kardar–Parisi–Zhang equation with flat initial conditions. Phys Rev Lett 2011;106(1–4):250603.
[88] Takeuchi KA. Crossover from growing to stationary interfaces in the Kardar–Parisi–Zhang class. Phys Rev Lett 2013;110(1–5):210604.
[89] Gallego R, Castro M, López J. Pseudospectral versus finite-difference schemes in the numerical integration of stochastic models of surface growth. Phys Rev E 2007;76(1–9):051121.
[90] Giada L, Giacometti A, Rossi M. Pseudospectral method for the Kardar–Parisi–Zhang equation. Phys Rev E 2002;65(1–11):036134.
[91] Gallego R. Predictor–corrector pseudospectral methods for stochastic partial differential equations with additive white noise. Appl Math Comput 2011;218:3905–17.
[92] H JD, Ermentrout B. Traveling waves in a spatially-distributed wilson–cowan model of cortex: From fronts to pulses. Physica D 2018;369:30–46.
[93] Seifert U. Stochastic thermodynamics, fluctuation theorems and molecular machines. Rep Progr Phys 2012;75:126001.
[94] Van den Broeck C. Stochastic thermodynamics: A brief introduction. In: Bechinger C, Sciortino F, Ziherl P, editors. Proc. Int. School Phys. Enrico Fermi - Course CLXXXIV Physics of Complex Colloids, IOS and SIF, Amsterdam and Bologna. 2013.
[95] Van den Broeck C, Esposito M. Ensemble and trajectory thermodynamics: A brief introduction. Physica A 2015;418:6–16.
[96] Seifert U. From stochastic thermodynamics to thermodynamic inference. Ann Rev Cond Matt Phys 2019;10:171–92.
[97] Jarzynski C. Equilibrium free-energy differences from nonequilibrium measurements: A master-equation approach. Phys Rev E 1997;56:5018.
[98] Chernyak V, Chertkov M, Jarzynski C. Path-integral analysis of fluctuation theorems for general Langevin processes. J Stat Mech: Theor Exp 2006;2006:P08001.
[99] Wio HS, Deza RR, Revelli JA. Fluctuation theorems and large-deviation functions in systems not featuring a steady state. J Stat Mech 2020;2020:024009.
[100] Rodríguez MA, Gallego R, Wio HS. Stochastic entropies and fluctuation theorems for a generic 1D KPZ system: Internal and external dynamics. Europhys.Lett. 2021;116:58005.

[101] Gingrich TR, Horowitz JM, Perunov N, England JL. Dissipation bounds all steady-state current fluctuations. Phys Rev Lett 2016;116:120601.
[102] Gingrich TR, Rotskoff GM, Horowitz JM. Inferring dissipation from current fluctuations. J Phys A 2017;50:184004.
[103] Horowitz JM, Gingrich TR. Thermodynamic uncertainty relations constrain non-equilibrium fluctuations. Nat Phys 2019;16:15–20.
[104] Seifert U. Stochastic thermodynamics: From principles to the cost of precision. Physica A 2018;504:176–91.
[105] Niggemann O, Seifert U. Field theoretic thermodynamic uncertainty relations: General formulation exemplified with the Kardar–Parisi–Zhang equation. J Stat Phys 2020;178:1142–74.
[106] Niggemann O, Seifert U. Numerical study of the thermodynamic uncertainty relation for the KPZ equation. J Stat Phys 2021a;182:25.
[107] Niggemann O, Seifert U. The two scaling regimes of the thermodynamic uncertainty relation for the KPZ equation. J Stat Phys 2021b;186:3.
[108] Hasegawa Y, Vu TV. Uncertainty relations in stochastic processes: An information inequality approach. Phys Rev E 2019;99:062126.
[109] Frieden BR, Gatenby RA, editors. Exploratory data analysis using fisher information. London: Springer; 2007.
[110] Tagliazucchi E, Balenzuela P, Fraiman D, Chialvo DR. Criticality in large-scale brain fmri dynamics unveiled by a novel point process analysis. Front Physiol 2012;4:15.
[111] Moretti P, noz MAM. Griffiths phases and the stretching of criticality in brain networks. Nat Comm 2013;3:2521.
[112] Pikovsky A, Zaikin A. System size stochastic and coherence resonance. AIP Conf Proc 2003;665:561–8.